Journal of Neurochemistry

JOURNAL OF NEUROCHEMISTRY | 2016 | 138 | 374–383 doi: 10.1111/jnc.13659

ORIGINAL ARTICLE

A voltammetric and mathematical analysis of histaminergic modulation of serotonin in the mouse hypothalamus

Srimal Samaranayake,* Aya Abdalla,* Rhiannon Robke,* H. Frederik Nijhout,† Michael C. Reed,‡ Janet Best§ and Parastoo Hashemi*

*Department of Chemistry and Biochemistry, University of South Carolina, Columbia, South Carolina, USA

†Department of Biology, Duke University, Durham, North Carolina, USA

‡Department of Mathematics, Duke University, Durham, North Carolina, USA

§Department of Mathematics, The Ohio State University, Columbus, Ohio, USA

Abstract

Histamine and serotonin are neuromodulators which facilitate numerous, diverse neurological functions. Being co-localized in many brain regions, these two neurotransmitters are thought to modulate one another's chemistry and are often implicated in the etiology of disease. Thus, it is desirable to interpret the *in vivo* chemistry underlying neurotransmission of these two molecules to better define their roles in health and disease. In this work, we describe a voltammetric approach to monitoring serotonin and histamine simultaneously in real time. Via electrical stimulation of the axonal bundles in the medial forebrain bundle, histamine release was evoked in the mouse premammillary nucleus. We found that histamine release was accompanied by a rapid, potent inhibition of serotonin in a concentration-dependent manner. We developed mathematical models to capture the experimental time courses of histamine and serotonin, which necessitated incorporation of an inhibitory receptor on serotonin neurons. We employed pharmacological experiments to verify that this serotonin inhibition was mediated by H_3 receptors. Our novel approach provides fundamental mechanistic insights that can be used to examine the full extent of interconnectivity between histamine and serotonin in the brain.

Keywords: carbon fiber microelectrodes, fast-scan cyclic voltammetry, H_3 autoreceptor, heteroreceptor, thioperamide.

J. Neurochem. (2016) **138**, 374–383.

Serotonin and histamine are neuromodulators thought to carry a variety of roles in the brain (Chase and Murphy 1973; Brown *et al.* 2001; Haas *et al.* 2008). These two modulators are co-localized in many brain regions (Moore *et al.* 1978; Russell *et al.* 1990) and are postulated to closely modulate one another (Laitinen *et al.* 1995; Threlfell *et al.* 2004). However, while there is much focus on serotonin's roles in affective, sleep and cognition processes (Portas *et al.* 2000; Cowen and Sherwood 2013), histamine's contribution to the same processes remains relatively neglected. In recent years, we established fast-scan cyclic voltammetry (FSCV) at carbon fiber microelectrodes (CFMs) to investigate *in vivo* serotonin dynamics (Hashemi *et al.* 2009). We are systematically studying the array of *in vivo* processes that regulate serotonin extracellular levels (Wood *et al.* 2014, 2015) with the ultimate goal of identifying distinct mechanistic abnormalities that underlie different pathophysiological states. Because of histamine's close association with serotonin, in particular the electrophysiological, histological, and slice voltammetry studies that imply histamine inhibits serotonin release (Hough 1988; Schlicker *et al.* 1988; Fink *et al.* 1990; Threlfell *et al.* 2004), we now find it of great importance to direct our efforts to voltammetrically defining histamine and serotonin co-modulation *in vivo*.

Received February 3, 2016; revised manuscript received April 12, 2016; accepted May 6, 2016.

Address correspondence and reprint requests to Parastoo Hashemi, Department of Chemistry and Biochemistry, University of South Carolina, Columbia, SC 29208, USA. E-mail: hashemi@mailbox.sc.edu

Abbreviations used: 5-HT, serotonin; CFMs, carbon fiber microelectrodes; CV, cyclic voltammogram; FIA, flow injection analysis; FSCV, fast-scan cyclic voltammetry; HA, histamine; MFB, medial forebrain bundle; PM, premammillary nucleus; SEM, standard error of the mean; SNr, substantia nigra pars reticulata.

In this paper, we extend on recent work where we described the first voltammetrically selective waveform for real-time FSCV histamine measurements *in vivo* in the mouse (Samaranayake *et al.* 2015), to detail simultaneous *in vivo* measurements of serotonin and histamine. To achieve this, CFMs were implanted in the mouse premammillary nucleus (PM), a hypothalamic region rich in serotonin and histamine (Moore *et al.* 1978; Russell *et al.* 1990; Marvin *et al.* 2010). To assess the effects of histamine release on endogenous serotonin chemistry, we identified a discrete location in the medial forebrain bundle (MFB) that, when electrically stimulated, evoked histamine but not serotonin in the PM. This robust experimental model allowed us to observe histamine release rapidly followed by potent, long-lasting serotonin inhibition. We found that both histamine release and serotonin inhibition were dependent on stimulation parameters in a manner that indicated an inversely correlative relationship. We mathematically modeled both responses and found that an inhibitory receptor term was necessary to fit both sets of data. We postulated that this inhibitory receptor was the H_3 receptor and provided pharmacological evidence, in the form of manipulations with thioperamide, an H_3 receptor antagonist, in favor of our hypothesis.

We thus provide not only an important technological advance, but our physiological findings also represent an opportunity to more closely scrutinize histamine's roles in controlling serotonin chemistry in the context of disease.

Materials and methods

Chemicals and reagents

Standard solutions were prepared by dissolving histamine dihydrochloride and serotonin hydrochloride (Sigma-Aldrich, Co., St. Louis, MO, USA), respectively, in Tris-buffer. Tris-buffer was constituted thus: 15 mM $H_2NC(CH_2OH)_2.HCl$, 140 mM NaCl, 3.25 mM KCl, 1.2 mM $CaCl_2$, 1.25 mM $NaH_2PO_4.H_2O$, 1.2 mM $MgCl_2$ and 2.0 mM Na_2SO_4 (EMD Chemicals Inc., Gibbstown, NJ, USA) in deionized water at pH = 7.4 thioperamide maleate (2, 20, or 200 mg/kg) from TOCRIS bioscience (Avonmouth, Bristol, UK) was dissolved in sterile saline and administered via intraperitoneal injection at a volume of 0.1 ml per 20 g of animal weight.

Carbon-fiber microelectrodes

CFMs were fabricated employing 7 μm diameter carbon-fibers (Goodfellow Corporation, Coraopolis, PA, USA) aspirated into glass capillaries (0.6 mm external diameter, 0.4 mm internal diameter; A-M Systems, Inc., Sequim, WA, USA). A carbon-glass seal was formed using a vertical micropipette puller (Narishige Group, Tokyo, Japan). The exposed length of the carbon fiber was trimmed to 150 μm under an optical microscope. Microelectrodes were electroplated with Nafion as described previously (Hashemi *et al.* 2009).

Data collection

Waveform generation, data acquisition, and signal processing were achieved by a commercial potentiostat (Dagan Corp. Minneapolis, MN, USA), custom-built hardware, software written in house using LabVIEW 2009, and interfacing a PCIe-6341 DAC/ADC card (National Instruments, Austin, TX, USA). Custom-built software was employed to drive the hardware and perform data analysis including background subtraction, signal averaging, and digital filtering (Knowmad Technologies LLC, Tucson, AZ, USA). All potentials are quoted with respect to Ag/AgCl reference electrodes, which were fabricated via electrodeposition of Cl^- by holding a silver wire (A-M Systems) at 4.0 V for 5 s in 1 M HCl. All data represented with error bars represent the standard error of the mean (SEM).

Data analysis

All the current versus time data were extracted from the custom-made software. Histamine current was transferred to its concentration using 2.825 μM/nA factor. The conversion factor for serotonin was 11 nM/nA. Statistical differences were obtained using one-tailed Student's *t*-tests on paired data sets. ($p < 0.05$ was taken as significantly different).

Data modeling

Simulations were carried out in MatLab R2014a (MathWorks, Natick, MA, USA) using ODE solver ode23s, implemented on an iMAC with operating system OS X Version 10.6.8. We modeled our experimental data with two differential equations:

$$\frac{d[\mathrm{eha}]}{\mathrm{dt}} = A_{\mathrm{H3}}(t)\mathrm{fire}_{\mathrm{ha}}(t)[\upsilon\mathrm{ha}] - V_{\mathrm{u}}([\mathrm{eha}]) + a_1[\mathrm{cha}] - V_{\mathrm{ug}}([\mathrm{eha}]) - a_2[\mathrm{gha}] \quad (1)$$

The left hand side is the rate of change of the extracellular histamine [eha]. The first term on the right side multiplies the fractional release, $A_{\mathrm{H3}}(t)$, caused by autoreceptor inhibition by the firing rate, $\mathrm{fire}_{\mathrm{ha}}(t)$, and the vesicular histamine concentration, [υha]. The remaining terms are reuptake into the terminal, $V_{\mathrm{u}}([\mathrm{eha}])$, leakage from the terminal, $a_1[\mathrm{cha}]$, uptake into glial cells, $V_{\mathrm{ug}}([\mathrm{eha}])$, and leakage from the glial cells, $a_2[\mathrm{gha}]$. There is a similar differential equation for serotonin in the extracellular space:

$$\frac{d[\mathrm{e5ht}]}{\mathrm{dt}} = A_{\mathrm{H3}}^{\mathrm{5ht}}(t)\mathrm{fire}_{\mathrm{5ht}}(t)[\mathrm{v5ht}] - V_{\mathrm{sert}}([\mathrm{e5ht}]) + a_3[\mathrm{c5ht}] - V_{\mathrm{ug}}([\mathrm{e5ht}]) - a_4[\mathrm{g5ht}] \quad (2)$$

The term $A_{\mathrm{H3}}^{\mathrm{5ht}}$ is the time course of fractional serotonin release caused by the H_3 receptors on serotonin neurons. All other terms in equation 2 are analogous to the terms in equation 1.

Flow injection analysis

Flow injection analysis was used for *in vitro* analyses. CFMs were inserted into a flangeless short 1/8 nut (PEEK P-335; IDEX, Middleboro, MA, USA) in order for 2 mm of the tip to be exposed outside of the nut. The microelectrode-containing nut was then fastened into a modified HPLC union elbow (PEEK 3432; IDEX). The other end of the elbow union was fastened into the out-flowing stream of the flow injection analysis buffer for a 'waste' flow stream and incorporation of the reference electrode by drilling into the union. *In vitro* experiments were carried out at 2 mL/min flow rate using syringe infusion pump (model KDS-410; KD Scientific, Holliston, MA, USA). Starting at 5 s, a rectangular pulse of analyte

was introduced into the buffer stream for 10 s via a six-port HPLC loop injector (Rheodyne model 7010 valve; VICI, Houston, TX, USA). In order to avoid carry-over effects, analytes were injected randomly.

Animal surgeries

Handling and surgery on male C57BL/6J mice weighing 20–25 g (Jackson Laboratory, Bar Harbor, ME, USA) were in agreement with the University of South Carolina Guide for the Care and Use of Laboratory Animals, approved by the Institutional Animal Care and Use Committee. Urethane (25% dissolved in 0.9% NaCl solution, Hospira, Lake Forest, IL, USA) was injected intraperitoneally (*i.p.*) and once deep anesthesia was confirmed, animals were secured into a stereotaxic instrument (David Kopf Instruments, Tujunga, CA, USA) and stereotaxic surgery was performed. A heating pad sustained mouse body temperature around 37°C (Braintree Scientific, Braintree, MA, USA). Stereotaxic coordinates were taken with reference to bregma. A Nafion modified CFM was implanted into the PM (AP: −2.45, ML: +0.50, DV: −5.45 to −5.55.). A stainless steel stimulating electrode (diameter: 0.2 mm; Plastics One, Roanoke, VA, USA) was positioned into the MFB (AP: −1.07, ML: +1.10, DV: −5.00). Biphasic pulse trains applied through a linear constant current stimulus isolator (NL800A, Neurolog; Medical Systems Corp., Great Neck, NY, USA) provoked histamine efflux. The 60 Hz trains were 360 μA each phase, 2 ms in width, and 2 s in length. To determine the effects of different stimulation parameters on histamine and serotonin, stimulation frequency, width, and amplitude were systematically altered. The time in between stimulations (2 min) was determined sufficient to produce negligible effects on serotonin and histamine in subsequent stimulations. A Ag/AgCl reference electrode (constructed by plating Cl^- ions onto a Ag wire) was implanted into the brain's opposite hemisphere.

Results

Simultaneous measurements of serotonin and histamine

In this experiment, we implanted a CFM in the PM of an anesthetized mouse and electrically stimulated the MFB. A representation of this experimental model, illustrating the relative positions of the working and stimulating electrodes can be found in Fig. 1(ai). Directly underneath this, in Fig. 1(bi), is a raw data color plot showing the resultant electrochemical signal at the CFM. The interpretation of color plots is described elsewhere in detail (Michael *et al.* 1999). Concisely, background-subtracted cyclic voltammograms collected at 10 Hz for 30 s are displayed as voltage (*y*-axis) versus time (*x*-axis) and current (false color). The green bar directly under the color plot denotes the occurrence and duration of the electrical stimulation. Upon stimulation there are several events, typical of *in vivo* FSCV measurements whereby other electroactive species, pH changes and ionic fluxes affect the measurement (Jones *et al.* 1994; Takmakov *et al.* 2010). Of interest is the discrete event occurring at 0.3 V which is denoted by the horizontal dashed line and the blue star. A cyclic voltammogram (CV) extracted from the vertical dashed line through this event is displayed in Fig. 1(ci) (solid line). The oxidation peak at 0.3 V shows excellent agreement with the oxidation peak extracted from an *in vitro* injection of histamine (dashed) normalized to maximum current and superimposed onto this *in vivo* CV. In our prior work, we showed electrochemically and pharmacologically that this event is histamine release (Samaranayake *et al.* 2015). Histamine's electro-oxidation scheme has not yet been described. It is likely that the peak at 0.3 V occurs because of a proton transfer type oxidation between the aliphatic amine group and imidazole amine group in the histamine molecule. Because this is an internal proton transfer oxidation, it follows that it should occur at a potential lower than that observed for classic serotonin and dopamine electro-oxidation (i.e. 0.6–0.8 V) (Hashemi *et al.* 2012).

An additional event of interest occurs at around 0.7 V and is denoted by the horizontal dashed line and red heart. Because FSCV is background subtracted, ambient levels cannot be determined, thus according to the false color scale, this event signals a decrease in concentration. A CV collected at the vertical dashed line through this event is presented in Fig. 1(cii). A CV taken from an *in vitro* injection of serotonin was inverted on the current axis (to mimic a decrease in concentration), normalized to maximum current, and superimposed (dashed) onto the *in vivo* CV. The good agreement between the peaks at 0.7 V strongly implies that this event is caused by serotonin. To further confirm this notion, we made a measurement of serotonin with this waveform via an experimental model of MFB stimulation and measurement in the substantia nigra pars reticulata (SNr) that we have well established for serotonin FSCV (Hashemi *et al.* 2011). This experimental model is depicted in Fig. 1(aii) and the color plot arising from the *in vivo* experiment is shown in Fig. 1(bii). The stimulated serotonin event occurs at the same horizontal (potential) position on the color plot. The CV extracted from this color plot, inverted, normalized to maximum current, and superimposed to the *in vivo* CV collected in the PM shows an excellent agreement in Fig. 1(ciii).

Serotonin inhibition following histamine release

The event immediately following histamine release proceeds in the negative false color current direction. FSCV cannot determine basal concentrations (*vide supra*); thus, one can only determine changes from ambient levels. This result, therefore, is indicative of a reduction in the ambient concentration of serotonin after stimulation. Figure 2(a) is a representative color plot showing simultaneous histamine release and serotonin inhibition in the PM upon MFB stimulation. Figure 2(c–e) shows serotonin and histamine concentrations with time for different stimulation parameters (dark solid lines = maximum responses and lighter dashed lines = lower responses) extracted from the horizontal dashed lines from the color plot ($n = 5$ animals). The decrease in serotonin concentration is delayed around 2 s

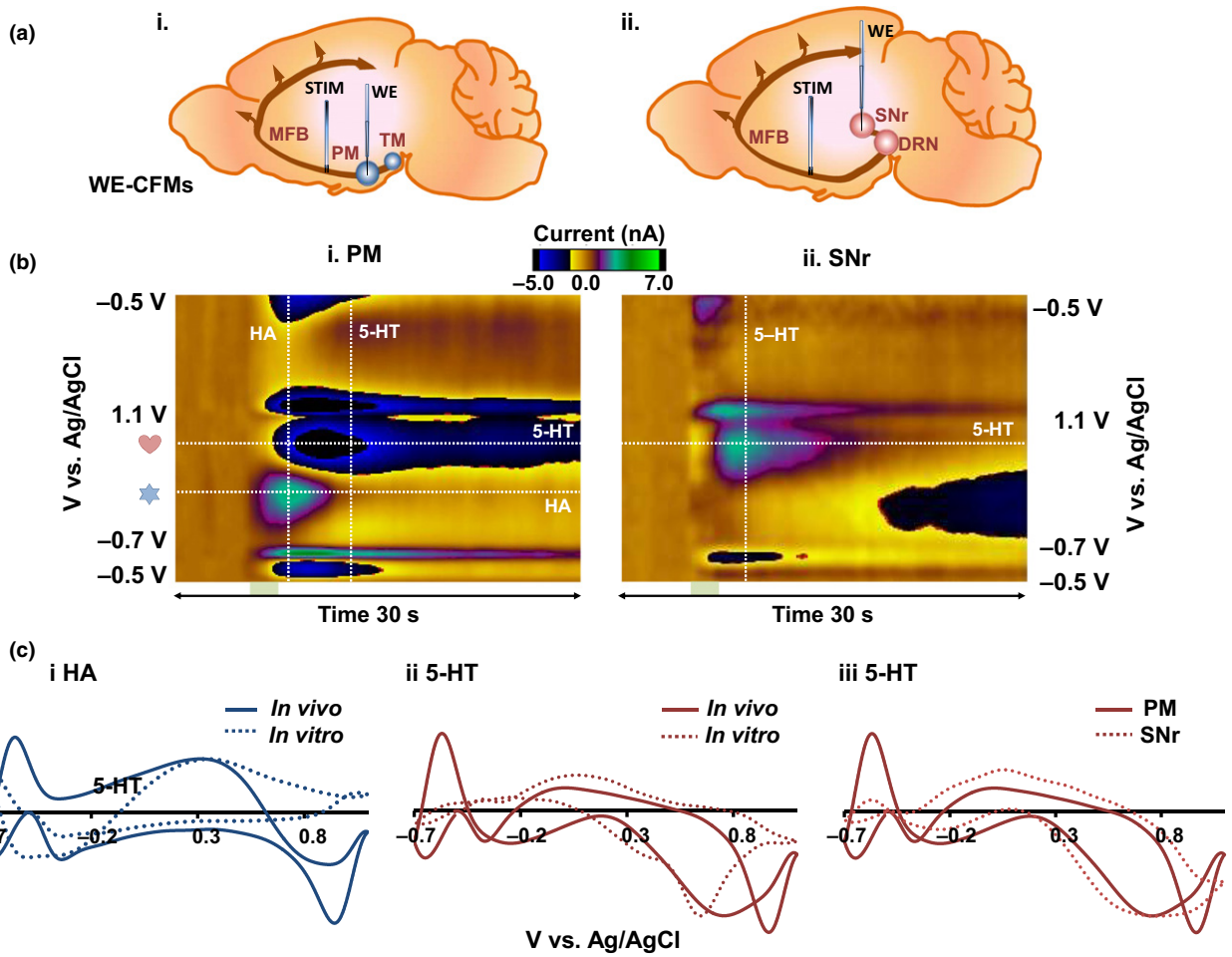

Fig. 1 (ai & aii) The position of electrodes (stimulation and carbon fiber microelectrodes) in the mouse brain. (bi & bii) Representative color plots of the stimulated release of histamine and serotonin in the premammillary nucleus (PM) and stimulated release of serotonin in the substantia nigra pars reticulata (SNr), respectively. (ci & ii) Superimposed cyclic voltammograms of *in vivo* and *in vitro* histamine and serotonin signals taken from vertical dashed lines in the PM. (ciii) Comparison of normalized cyclic voltammograms of *in vivo* serotonin signals taken from vertical dashed lines in both PM and SNr. HA, histamine; 5-HT, serotonin.

with respect to histamine release, implying that serotonin inhibition may be dependent on histamine release. To probe this notion, we systematically altered stimulation parameters to assess whether the profile of histamine release affects serotonin inhibition. The dark solid line shows the maximum responses for the 60 Hz stimulation frequency in Fig. 2(c). The lighter colored dashed lines in Fig. 2(c) shows the result of altering the stimulation frequency from 10 to 40 Hz ($n = 5$ animals). There is a clear correlation between histamine release and the serotonin inhibition profiles. This is apparent in terms of both time course (i.e. 10 Hz stimulation leading to lower, more prolonged histamine release and subsequent serotonin inhibition) and amplitude (higher level of histamine release corresponds to higher level of serotonin inhibition). This pattern holds true for stimulation pulse width and amplitude (Fig. 2d and e) ($n = 5$ animals). In Fig. 2(b), the relationship between histamine release and serotonin inhibition was more formally explored by directly plotting amplitude of histamine release versus amplitude of serotonin inhibition for the three stimulation parameters explored. We found a linear relationship ($R^2 = 0.757$) connecting histamine release to serotonin inhibition for all three parameters explored.

Mathematical modeling of serotonin and histamine co-regulation

We needed to vary only three functions, $\text{fire}_{\text{ha}}(t)$, $A_{\text{H3}}(t)$, and $A_{\text{H3}}^{5\text{ht}}(t)$, from equations 1 and 2 to obtain an excellent model that fits our experimental data. Figure 3(a and b) show the model fits (dotted lines) to the experimental curves (solid lines) of histamine and serotonin for control and 20 mg/kg thioperamide, respectively. Thioperamide selectively acts as an H_3 receptor (auto and hetero) antagonist on both histamine and serotonin pre-synaptic neurons (Bernaerts *et al.* 2004).

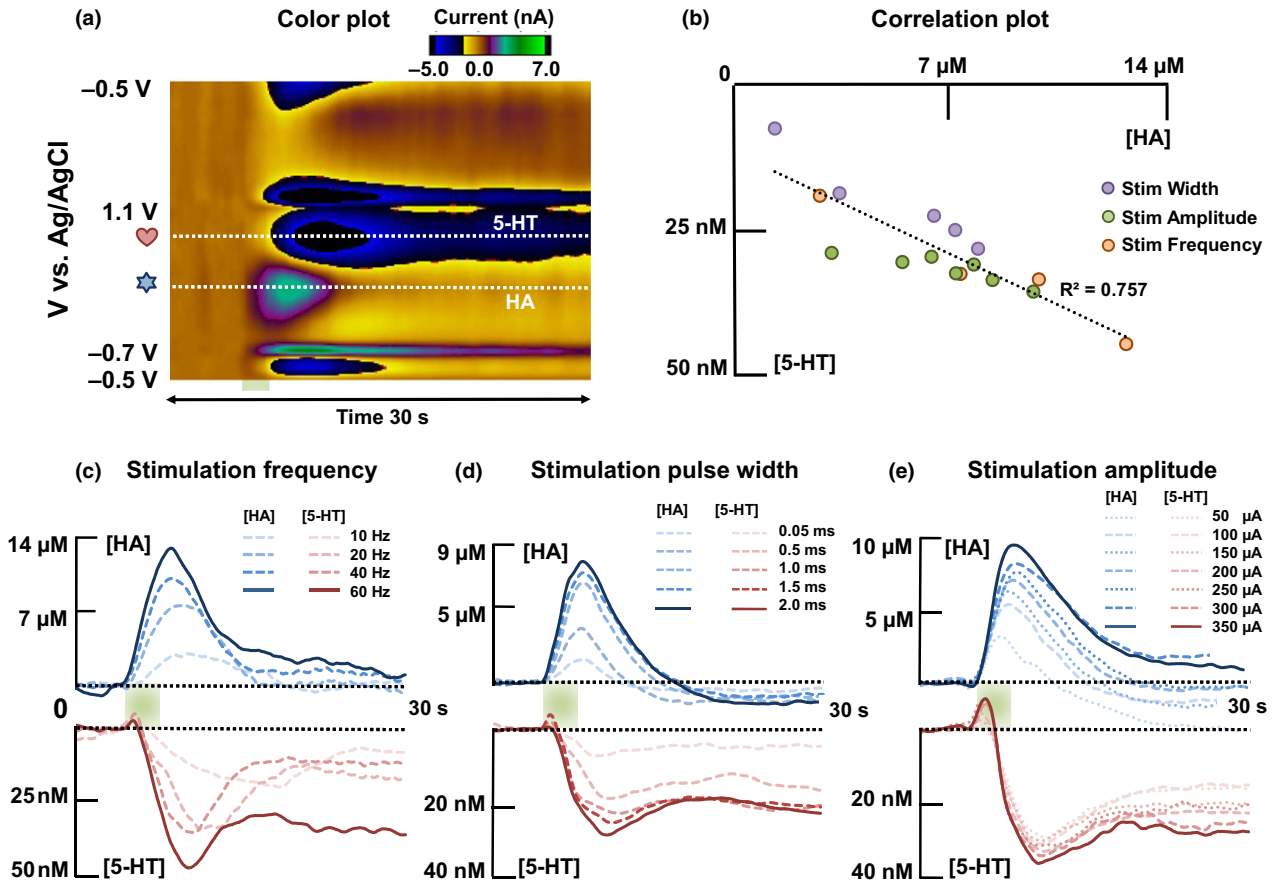

Fig. 2 (a) Representative color plot of the stimulated release of histamine and serotonin inhibition in the premammillary nucleus. (b) Correlation plot between [histamine] and [serotonin] for all stimulation parameters. (c) Averaged current versus time traces along the two horizontal dashed lines of histamine and serotonin with respect to different stimulation frequencies ($n = 5$). (d) Averaged current responses to various stimulation pulse widths of histamine and serotonin ($n = 5$). (e) Averaged current responses to various stimulation amplitudes of histamine and serotonin ($n = 5$). HA, histamine; 5-HT, serotonin.

In our model, the electrical stimulation is mimicked by raising $\text{fire}_{\text{ha}}(t)$ above its tonic level of 5 spikes/sec. Figure 3(c) shows $\text{fire}_{\text{ha}}(t)$ versus time that best fits the control and thioperamide experiments. $\text{fire}_{\text{ha}}(t)$ returns to baseline at 9 s and the rates are higher after thioperamide.

To fit the slow decline in histamine after stimulation, it was necessary to incorporate an autoreceptor function as per our previous serotonin model (Wood *et al.* 2014) Fig. 3(d) shows fractional histamine release, $A_{\text{H3}}(t)$, as a function of H_3 autoreceptor activation following stimulation before and after thioperamide. In the control experiment, tonic inhibition was $A_{\text{H3}}(t) = 0.7$ up to 9 s, then dropped to $A_{\text{H3}}(t) = 0$ up to 15 s (complete inhibition), and then returned to $A_{\text{H3}}(t) = 0.4$ from 15 s to 30 s. For thioperamide, $A_{\text{H3}}(t) = 0.9$, and the smallest fractional release is $A_{\text{H3}}(t) = 0.5$. Our model shows that the H_3 autoreceptor effect is delayed (starting at 9 s) and lasts throughout our file collection window (30 s).

We next modeled our serotonin curves. Since the serotonin neurons are not stimulated, $\text{fire}_{\text{5ht}}(t)$ remains at a tonic level of 5 spikes/sec. We varied $A_{\text{H3}}^{\text{5ht}}(t)$ (fraction of serotonin release permitted by the H_3 receptors on serotonin neurons). For the control experiment, $A_{\text{H3}}^{\text{5ht}}(t)$ starts at 0.9, goes down to 0.45, and then returns to 0.9. For thioperamide, $A_{\text{H3}}^{\text{5ht}}(t)$ starts at 0.9, goes down to 0.36, and then returns to 0.8 at 30 s (graphs not shown). As above, the H_3 receptor effect is prolonged throughout file collection (> 60 s).

H_3 Receptor mediated inhibition of serotonin

Three different doses of thioperamide, an H_3 receptor antagonist (Bernaerts *et al.* 2004), were administered to different groups of mice. This agent's effects on histamine release and serotonin inhibition was observed 50 min after administration, which is a sufficient time period for thioperamide to exert its effects (Bordi *et al.* 1992; Akhtar *et al.* 2005). The results are shown in Fig. 4. Here, histamine before drug is displayed in blue and after drug in green, serotonin before drug is red, and after drug is orange. Error bars showing SEM ($n = 5 \pm$ SEM) are lighter versions of these respective colors.

Thioperamide, administered at 2 mg/kg caused a significant increase in the amplitude of histamine release from 7.5 ± 1.4 μM to 11.5 ± 1.4 μM (p = 0.004), but not in the rate of histamine clearance ($t_{1/2}$ from 11.5 ± 1.5 s to 14.3 ± 2.4 s, p = 0.07). The effects of 2 mg/kg on the amplitude and time course of serotonin inhibition were negligible. Maximum serotonin inhibition changed from 34.2 ± 7.5 nM to 37.5 ± 11.9 nM (p = 0.55), whereas inhibition at 30 s enhanced from 15.8 ± 1.5 nM to 22.1 ± 8.9 nM (p = 0.31). Thioperamide administered at

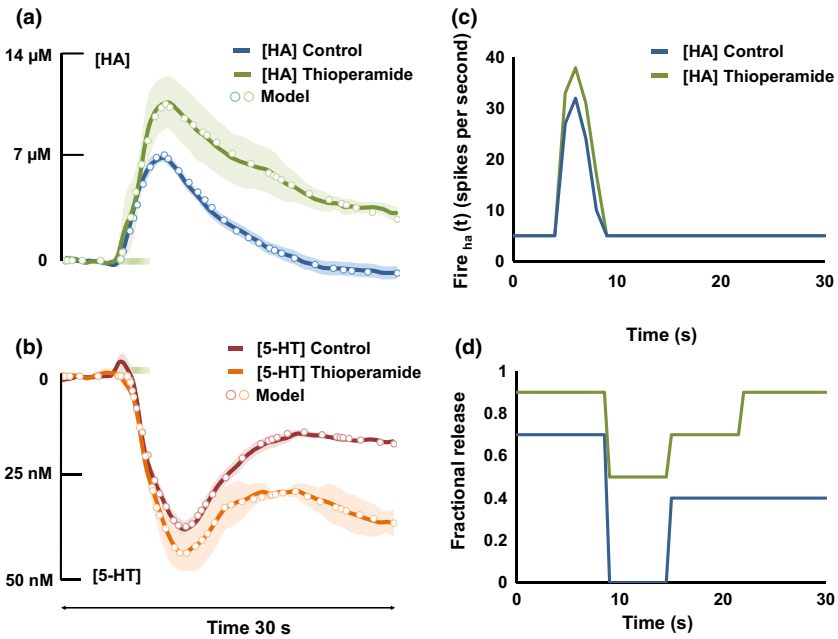

Fig. 3 (a) [Histamine] versus time plots comparing *in vivo* (solid traces) and the results of the mathematical model (large dots) in the control case. (b) [Serotonin] versus time plots comparing *in vivo* (solid traces) and the results of the mathematical model (large dots) in the presence of thioperimide (20 mg/kg) (c) Firing rate of the histamine neurons as a function of time in the two cases control (blue) and drug (green), respectively. (d) Assumed fractional release of histamine from the histamine neurons as a function of time in the two cases. HA, histamine; 5-HT, serotonin.

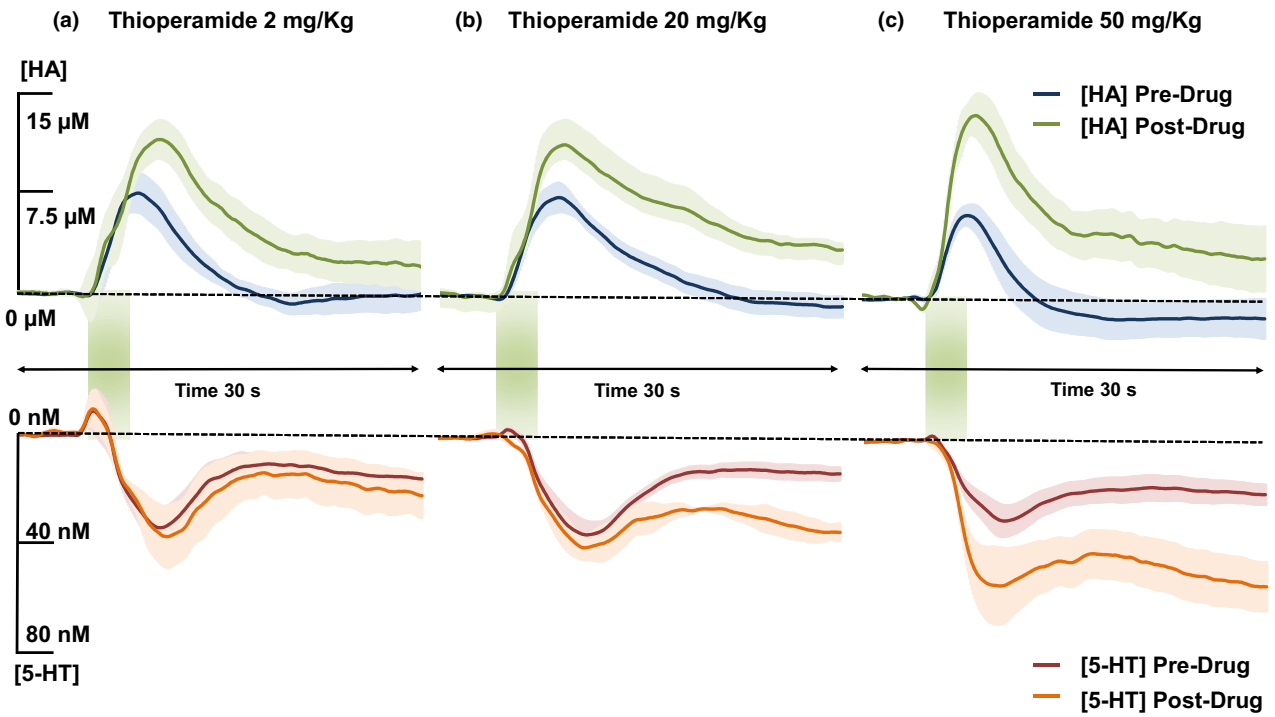

Fig. 4 [Histamine] versus time traces are shown in blue and green for pre- and post-drug administration, respectively. [Serotonin] versus time traces are shown in red and orange for before and after the drug respectively. Error bars showing SEM (n = 5 ± SEM) are lighter versions of these respective colors. (a) thioperamide 2 mg/kg (b) thioperamide 20 mg/kg (c) thioperamide 50 mg/kg. HA, histamine; 5-HT, serotonin.

20 mg/kg affected both the amplitude and clearance time of histamine response. Histamine release is elevated from 7.9 ± 2.1 μM to 11.9 ± 4.2 μM ($p = 0.03$) and $t_{1/2}$ increased from 14.7 ± 2.8 s to 19.6 ± 2.3 s ($p = 0.02$), but only the time course of the serotonin response (maximum inhibition from 38.8 ± 5.01 nM to 44.8 ± 4.5 nM ($p = 0.31$). Furthermore, serotonin inhibition at 30 s increases from 16.5 ± 5.3 nM to 37.7 ± 9.6 nM, ($p = 0.002$). At the highest dose, thioperamide greatly affected histamine release from 6.8 ± 1.9 μM to 14.3 ± 4.1 μM ($p = 0.006$) and reuptake such that histamine does not return to baseline during the 30 s file acquisition window. The effects on serotonin are also highly significant. Maximum inhibition elevated from 37.3 ± 9.6 nM to 68.2 ± 20.0 nM ($p = 0.04$), whereas inhibition at 30 s enhanced from 24.4 ± 7.9 nM to 65.9 ± 14.8 nM ($p = 0.03$).

Discussion

FSCV: a powerful tool for simultaneous, real-time serotonin and histamine measurements

Fast-scan cyclic voltammetry at CFMs is a powerful tool for neurotransmitter analysis because of FSCV's rapid, sensitive, and selective analysis capabilities, in addition to the minimally invasive dimensions of CFMs. A traditional drawback of FSCV is its limited *in vivo* analytical scope (measuring primarily dopamine) (Millar *et al.* 1985; Zhou *et al.* 2001; Montague *et al.* 2004), which has been systematically challenged in recent years via advances to measure serotonin (Hashemi *et al.* 2009), adenosine (Swamy and Venton 2007), H_2O_2 (Sanford *et al.* 2010), and gonadotropin-releasing hormone (Glanowska *et al.* 2012). We are primarily interested in deciphering the *in vivo* dynamics that regulate extracellular serotonin levels, and we were thus oriented toward histamine. There is a significant body of literature that suggests histamine inversely modulates serotonin in the brain (Schlicker *et al.* 1988; Threlfell *et al.* 2004). Many of these studies propose that dysregulations in histamine underlie disorders that are primarily considered to be serotonin mediated (e.g. depression) (Barbeau 1962; Schneider *et al.* 1997; Muller *et al.* 2007). In 2011, we described simultaneous histamine and serotonin measurements in the rat SNr (Hashemi *et al.* 2011). However, the FSCV peaks utilized to quantify histamine occurred at the anodic switching potential. These so-called 'switching peaks' occur when spontaneous adsorption of analytes changes the electrical bilayer; hence, creates capacitative current on the CFM. While switching peaks can be used to quantify histamine in a well-controlled environment (i.e. *in vitro* or tissue slice preparations), they cannot be used *in vivo* because other analytes that adsorb to the CFM provide identical, indistinguishable CVs (Samaranayake *et al.* 2015).

In 2015, we addressed the issue of selective *in vivo* histamine analysis by developing a detection waveform that displayed a distinct Faradaic-like peak corresponding to histamine oxidation. We successfully applied this waveform *in vivo* to selectively quantify histamine (Samaranayake *et al.* 2015). In this study, we show that this novel waveform can simultaneously and selectively measure not only histamine but also serotonin (*vide infra*), which greatly aids our interests in establishing how histamine modulates serotonin chemistry.

MFB stimulation rapidly, potently inhibits ambient serotonin in the PM

Figure 1 shows histamine release upon MFB stimulation in a hypothalamic region, the PM. We and others previously established this stimulation and measurement model to be robust and successful in evoking histamine (Panula *et al.* 1984; Rozov *et al.* 2014) since the PM is home to a dense population of histamine cell bodies (Panula *et al.* 1984) and the region of the MFB that we stimulate contains histamine axons (Garbarg *et al.* 1974; Auvinen and Panula 1988). The PM region also contains serotonin terminals (Moore *et al.* 1978; Marvin *et al.* 2010), therefore, we postulated that the PM seemed a promising area to study histamine/serotonin modulation, particularly because our data imply that the electrical stimulation does not evoke serotonin. This finding is supported by the presence of fewer serotonin axons in the anterior area of the MFB (our stimulation location) (Nieuwenhuys *et al.* 1982; Veening *et al.* 1982). Importantly, this model allows us to investigate histamine's effects on serotonin chemistry in the absence of stimulated serotonin release. This type of measurement can be greatly facilitated in the future with the development of optogenetic tools that selectively target histamine.

In accord with our postulation, in Fig. 1, an event following the evoked histamine event by around 2 s is apparent. Via comparison of CVs collected *in vitro* and *in vivo* in the SNr (an area we have well established for serotonin FSCV) (Hashemi *et al.* 2012; Dankoski and Wightman 2013), we can electrochemically verify this second event to be caused by serotonin. The small deviation in the peak positions in Fig. 1(cii) is typical when comparing *in vivo* and *in vitro* responses and is likely because of differences in ohmic drop between *in vitro* and *in vivo* preparations. Of great interest, our data indicate that the serotonin levels are *decreasing* in response to the stimulation. Because FSCV is a background subtracted method, ambient levels cannot be established; therefore, the conclusion of this data is that MFB stimulation inhibits ambient serotonin activity by around 40 nM. FSCV most commonly observes increased neurotransmitter activity, thus our experiment represents an exciting opportunity to study inhibition of ambient activity.

We next hypothesize that this inhibition is, at least partially, mediated by histamine based on prior histamine/serotonin modulation studies (Schlicker *et al.* 1988; Threlfell *et al.* 2004). In the next sections, we take experimental,

mathematical, and pharmacological approaches toward this hypothesis.

Histamine mediates serotonin inhibition in the PM

Serotonin inhibition is concentration and time correlated with histamine release

To show that histamine, rather than another result of MFB stimulation inhibits serotonin in the PM, we systematically altered our stimulation parameters to change the profile of histamine release. Figure 2 shows excellent agreement between the time course and amplitude of histamine release and serotonin inhibition. The raw data in Fig. 2(c–e) show that the profile of serotonin inhibition closely tracks histamine release, and the Fig. 2(b) highlights this correlation more formally by plotting maximum histamine release amplitude versus maximum serotonin inhibition amplitude. The linear relationship between histamine and serotonin with all stimulation parameters is strong evidence for chemical rapport between these two molecules in the PM.

Mathematical modeling of serotonin inhibition necessitates an autoreceptor function

The power of interpreting experimental data through mathematical models is the ability to test a number of physiological hypotheses. Above, we hypothesized that serotonin inhibition is histamine mediated, and we now test this notion mathematically. Our model necessitates ambient (basal) histamine and serotonin levels which we are not yet able to determine with FSCV. For histamine, a value of 1.5 μM was chosen because our data show that after stimulation histamine levels fall 1 μM or more below baseline (Figs 2, 3 and 4). Similarly, for the same reason we chose 65 nM as the basal concentration of serotonin in the extracellular space. We found that we could fit the data closely via simple manipulations of H_3 heteroreceptor and autoreceptor strengths in our model. H_3 heteroreceptors on serotonin terminals (Schlicker *et al.* 1988; Esbenshade *et al.* 2008) have previously been postulated to inhibit serotonin (Threlfell *et al.* 2004). Our model supports this hypothesis, particularly given that is unlikely that the serotonin inhibition we observe is attributable to other slower mechanisms such as synthesis inhibition. Thus, to probe this idea further, we took a pharmacological approach.

H_3 receptor mediation of serotonin inhibition

Given the results of our mathematical modeling and the large body of prior work implicating H_3 heteroreceptors as an inhibitory mechanism for serotonin (Schlicker *et al.* 1988; Esbenshade *et al.* 2008), we decided to probe H_3 receptor mediation of serotonin. Figure 4 shows the results of systemically administering varying doses of a potent H_3 receptor antagonist, thioperamide, to different mice. The low dose (2 mg/kg) increased the amplitude of histamine release (consistent with prior studies with dopamine and D2 autoreceptor antagonism) (Clark *et al.* 1995; Kita *et al.* 2007), but has no significant effect on serotonin. This phenomenon is not difficult to explain because the serotonin response is controlled by dual mechanisms of a) now increased histamine available to antagonize H_3 receptors and b) a larger percentage of H_3 receptors antagonized on serotonin neurons. The overall result is a manifestation of two opposing effects that cancel each other out.

The 20 mg/kg dose had effects on both histamine release and clearance (reuptake effects have been previously been seen with serotonin autoreceptor antagonism) (Wood *et al.* 2014). The effect on the magnitude of serotonin inhibition was not significant; however, it seems that the prolonged histamine in the synapse is outcompeting thioperamide for H_3 receptors on serotonin neurons to create prolonged serotonin inhibition (> 60 s).

H_3 heteroreceptors are likely more localized in the synapse because of their position on serotonin terminals (Carlsson and Carlsson 2006) than are H_3 autoreceptors on pre-synaptic histamine neurons. Autoreceptors are generally found outside the direct synaptic space, asserting inhibition when a concentration threshold is reached (Langer *et al.* 2013). The inhibition constant (K_i) of thioperamide is smaller than the Michaelis Menten constant (K_m) of histamine toward H_3 receptors (Chen *et al.* 2003; Liedtke *et al.* 2003). However, after stimulation, histamine concentrations are very high in the direct synaptic space (likely reaching mMs based on prior dopamine models) (Garris *et al.* 1994) and fall off exponentially with distance. Because the thioperamide concentration is assumed to be homogenous throughout this brain region, the histamine most certainly outcompetes thioperamide for H_3 heteroreceptors on serotonin neurons. This notion is made apparent by the largest dose (50 mg/kg) of thioperamide which created significant and long-lasting serotonin inhibition.

In sum, we showcased the power of FSCV for simultaneous measurements of histamine and serotonin in the PM. We demonstrated that MFB stimulation released histamine but created a potent inhibition of serotonin. Voltammetrically, mathematically, and pharmacologically, we showed serotonin inhibition was dependent on histamine release, via an H_3 receptor-mediated mechanism. Our approach signals a powerful advancement in FSCV technology that will facilitate the systematic study of histamine and serotonin dynamics in the variety of different brain processes involving these two molecules.

Acknowledgments and conflict of interest disclosure

The authors thank Glenn Dryhurst and Eberhard Schlicker for helpful insights into histamine electro-oxidation and H_3 receptor K_i, respectively. The University of South Carolina start-up funds and

the Eli Lily Young Investigator Award in Analytical Chemistry to PH and an NSF award, DMS-0931642, and a NSF CAREER Award, DMS-0956057, to JB funded this research. The authors have no conflict of interest to declare.

All experiments were conducted in compliance with the ARRIVE guidelines.

References

Akhtar M., Pillai K. K. and Vohora D. (2005) Effect of thioperamide on modified forced swimming test-induced oxidative stress in mice. *Basic Clin. Pharmacol. Toxicol.* **97**, 218–221.

Auvinen S. and Panula P. (1988) Development of histamine-immunoreactive neurons in the rat brain. *J. Comp. Neurol.* **276**, 289–303.

Barbeau A. (1962) The pathogenesis of Parkinson's disease: a new hypothesis. *Can. Med. Assoc. J.* **87**, 802–807.

Bernaerts P., Lamberty Y. and Tirelli E. (2004) Histamine H3 antagonist thioperamide dose-dependently enhances memory consolidation and reverses amnesia induced by dizocilpine or scopolamine in a one-trial inhibitory avoidance task in mice. *Behav. Brain Res.* **154**, 211–219.

Bordi F., Mor M., Plazzi P. V., Silva C., Caretta A. and Morini G. (1992) HPLC detection of thioperamide from biological samples and its determination in rat blood and brain after systemic administration. *Farmaco*, **47**, 1095–1103.

Brown R. E., Stevens D. R. and Haas H. L. (2001) The physiology of brain histamine. *Prog. Neurobiol.* **63**, 637–672.

Carlsson A. and Carlsson M. L. (2006) A dopaminergic deficit hypothesis of schizophrenia: the path to discovery. *Dialogues Clin. Neurosci.* **8**, 137–142.

Chase T. N. and Murphy D. L. (1973) Serotonin and central nervous system function. *Annu. Rev. Pharmacol.* **13**, 181–197.

Chen J., Liu C. and Lovenberg T. W. (2003) Molecular and pharmacological characterization of the mouse histamine H3 receptor. *Eur. J. Pharmacol.* **467**, 57–65.

Clark D., Exner M., Furmidge L. J., Svensson K. and Sonesson C. (1995) Effects of the dopamine autoreceptor antagonist (-)-DS121 on the discriminative stimulus properties of d-amphetamine and cocaine. *Eur. J. Pharmacol.* **275**, 67–74.

Cowen P. and Sherwood A. C. (2013) The role of serotonin in cognitive function: evidence from recent studies and implications for understanding depression. *J. Psychopharmacol.* **27**, 575–583.

Dankoski E. C. and Wightman R. M. (2013) Monitoring serotonin signaling on a subsecond time scale. *Front. Integr. Neurosci.* **7**, 44.

Esbenshade T. A., Browman K. E., Bitner R. S., Strakhova M., Cowart M. D. and Brioni J. D. (2008) The histamine H3 receptor: an attractive target for the treatment of cognitive disorders. *Br. J. Pharmacol.* **154**, 1166–1181.

Fink K., Schlicker E., Neise A. and Gothert M. (1990) Involvement of presynaptic H3 receptors in the inhibitory effect of histamine on serotonin release in the rat brain cortex. *Naunyn Schmiedebergs Arch. Pharmacol.* **342**, 513–519.

Garbarg M., Barbin G., Feger J. and Schwartz J. C. (1974) Histaminergic pathway in rat brain evidenced by lesions of the medial forebrain bundle. *Science* **186**, 833–835.

Garris P. A., Ciolkowski E. L., Pastore P. and Wightman R. M. (1994) Efflux of dopamine from the synaptic cleft in the nucleus accumbens of the rat brain. *J. Neurosci.* **14**, 6084–6093.

Glanowska K. M., Venton B. J. and Moenter S. M. (2012) Fast scan cyclic voltammetry (FSCV) as a novel method for detection of real time gonadotropin-releasing hormone (GnRH) release in mouse brain slices. *J. Neurosci.* **32**, 14664–14669.

Haas H. L., Sergeeva O. A. and Selbach O. (2008) Histamine in the nervous system. *Physiol. Rev.* **88**, 1183–1241.

Hashemi P., Dankoski E. C., Petrovic J., Keithley R. B. and Wightman R. M. (2009) Voltammetric detection of 5-hydroxytryptamine release in the rat brain. *Anal. Chem.* **81**, 9462–9471.

Hashemi P., Dankoski E. C., Wood K. M., Ambrose R. E. and Wightman R. M. (2011) In vivo electrochemical evidence for simultaneous 5-HT and histamine release in the rat substantia nigra pars reticulata following medial forebrain bundle stimulation. *J. Neurochem.* **118**, 749–759.

Hashemi P., Dankoski E. C., Lama R., Wood K. M., Takmakov P. and Wightman R. M. (2012) Brain dopamine and serotonin differ in regulation and its consequences. *Proc. Natl Acad. Sci. USA* **109**, 11510–11515.

Hough L. B. (1988) Cellular localization and possible functions for brain histamine: recent progress. *Prog. Neurobiol.* **30**, 469–505.

Jones S. R., Mickelson G. E., Collins L. B., Kawagoe K. T. and Wightman R. M. (1994) Interference by pH and Ca2 + ions during measurements of catecholamine release in slices of rat amygdala with fast-scan cyclic voltammetry. *J. Neurosci. Methods* **52**, 1–10.

Kita J. M., Parker L. E., Phillips P. E., Garris P. A. and Wightman R. M. (2007) Paradoxical modulation of short-term facilitation of dopamine release by dopamine autoreceptors. *J. Neurochem.* **102**, 1115–1124.

Laitinen K. S. M., Tuomisto L. and Laitinen J. T. (1995) Endogenous serotonin modulates histamine release in the rat hypothalamus as measured by in vivo microdialysis. *Eur. J. Pharmacol.* **285**, 159–164.

Langer S. Z., Galzin A. M. and Costentin J. (2013) *Presynaptic Receptors and Neuronal Transporters: Official Satellite Symposium to the IUPHAR 1990 Congress Held in Rouen, France, on 26–29 June 1990*. Elsevier Science, Cambridge, MA.

Liedtke S., Flau K., Kathmann M., Schlicker E., Stark H., Meier G. and Schunack W. (2003) Replacement of imidazole by a piperidine moiety differentially affects the potency of histamine H3-receptor antagonists. *Naunyn Schmiedebergs Arch. Pharmacol.* **367**, 43–50.

Marvin E., Scrogin K. and Dudas B. (2010) Morphology and distribution of neurons expressing serotonin 5-HT1A receptors in the rat hypothalamus and the surrounding diencephalic and telencephalic areas. *J. Chem. Neuroanat.* **39**, 235–241.

Michael D. J., Joseph J. D., Kilpatrick M. R., Travis E. R. and Wightman R. M. (1999) Improving data acquisition for fast-scan cyclic voltammetry. *Anal. Chem.* **71**, 3941–3947.

Millar J., Stamford J. A., Kruk Z. L. and Wightman R. M. (1985) Electrochemical, pharmacological and electrophysiological evidence of rapid dopamine release and removal in the rat caudate nucleus following electrical stimulation of the median forebrain bundle. *Eur. J. Pharmacol.* **109**, 341–348.

Montague P. R., McClure S. M., Baldwin P. R., Phillips P. E., Budygin E. A., Stuber G. D., Kilpatrick M. R. and Wightman R. M. (2004) Dynamic gain control of dopamine delivery in freely moving animals. *J. Neurosci.* **24**, 1754–1759.

Moore R. Y., Halaris A. E. and Jones B. E. (1978) Serotonin neurons of the midbrain raphe: ascending projections. *J. Comp. Neurol.* **180**, 417–438.

Muller C. P., Carey R. J., Huston J. P. and De Souza Silva M. A. (2007) Serotonin and psychostimulant addiction: focus on 5-HT1A-receptors. *Prog. Neurobiol.* **81**, 133–178.

Nieuwenhuys R., Geeraedts L. M. and Veening J. G. (1982) The medial forebrain bundle of the rat. I. General introduction. *J. Comp. Neurol.* **206**, 49–81.

Panula P., Yang H. Y. and Costa E. (1984) Histamine-containing neurons in the rat hypothalamus. *Proc. Natl Acad. Sci. USA* **81**, 2572–2576.

Portas C. M., Bjorvatn B. and Ursin R. (2000) Serotonin and the sleep/wake cycle: special emphasis on microdialysis studies. *Prog. Neurobiol.* **60**, 13–35.

Rozov S. V., Zant J. C., Karlstedt K., Porkka-Heiskanen T. and Panula P. (2014) Periodic properties of the histaminergic system of the mouse brain. *Eur. J. Neuorsci.* **39**, 218–228.

Russell W. L., Henry D. P., Phebus L. A. and Clemens J. A. (1990) Release of histamine in rat hypothalamus and corpus striatum in vivo. *Brain Res.* **512**, 95–101.

Samaranayake S., Abdalla A., Robke R., Wood K. M., Zeqja A. and Hashemi P. (2015) In vivo histamine voltammetry in the mouse premammillary nucleus. *Analyst* **140**, 3759–3765.

Sanford A. L., Morton S. W., Whitehouse K. L., Oara H. M., Lugo-Morales L. Z., Roberts J. G. and Sombers L. A. (2010) Voltammetric detection of hydrogen peroxide at carbon fiber microelectrodes. *Anal. Chem.* **82**, 5205–5210.

Schlicker E., Betz R. and Gothert M. (1988) Histamine H3 receptor-mediated inhibition of serotonin release in the rat brain cortex. *Naunyn Schmiedebergs Arch. Pharmacol.* **337**, 588–590.

Schneider C., Risser D., Kirchner L., Kitzmuller E., Cairns N., Prast H., Singewald N. and Lubec G. (1997) Similar deficits of central histaminergic system in patients with Down syndrome and Alzheimer disease. *Neurosci. Lett.* **222**, 183–186.

Swamy B. E. and Venton B. J. (2007) Subsecond detection of physiological adenosine concentrations using fast-scan cyclic voltammetry. *Anal. Chem.* **79**, 744–750.

Takmakov P., Zachek M. K., Keithley R. B., Bucher E. S., McCarty G. S. and Wightman R. M. (2010) Characterization of local pH changes in brain using fast-scan cyclic voltammetry with carbon microelectrodes. *Anal. Chem.* **82**, 9892–9900.

Threlfell S., Cragg S. J., Kallo I., Turi G. F., Coen C. W. and Greenfield S. A. (2004) Histamine H3 receptors inhibit serotonin release in substantia nigra pars reticulata. *J. Neurosci.* **24**, 8704–8710.

Veening J. G., Swanson L. W., Cowan W. M., Nieuwenhuys R. and Geeraedts L. M. (1982) The medial forebrain bundle of the rat. II. An autoradiographic study of the topography of the major descending and ascending components. *J. Comp. Neurol.* **206**, 82–108.

Wood K. M., Zeqja A., Nijhout H. F., Reed M. C., Best J. and Hashemi P. (2014) Voltammetric and mathematical evidence for dual transport mediation of serotonin clearance in vivo. *J. Neurochem.* **130**, 351–359.

Wood K. M., Cepeda D. and Hashemi P. (2015) Probing serotonin neurotransmission: implications for neuropsychiatric disorders, in *Compendium of in Vivo Monitoring in Real-Time Molecular Neuroscience Vol 1: Fundamentals and Applications* (Wilson G.S. and Michael A.C., eds), pp. 269–285. Hackensack, NJ.

Zhou F. M., Liang Y. and Dani J. A. (2001) Endogenous nicotinic cholinergic activity regulates dopamine release in the striatum. *Nat. Neurosci.* **4**, 1224–1229.